

## Paper

Int'l J. of Aeronautical & Space Sci. 14(1), 58–66 (2013)  
DOI:10.5139/IJASS.2013.14.1.58

# Performance Comparison of Three Different Types of Attitude Control Systems of the Quad-Rotor UAV to Perform Flip Maneuver

**Byung-Yoon Lee\***, **Dong-Wan Yoo\*\*** and **Min-Jea Tahk\*\*\***

*Korea Advanced Institute of Science and Technology, Daejeon, Republic of Korea*

## Abstract

This paper addresses the performance of three different types of attitude control systems for the Quad-rotor UAV to perform the flip maneuver. For this purpose, Quad-rotor UAV's 6-DOF dynamic model is derived, and it was used for designing an attitude controller of the Quad-rotor UAV. Attitude controllers are designed by three different methods. One is the open-loop control system design, another is the PD control system design, and the last method is the sliding mode control system design. Performances of all controllers are tested by 6-DOF simulation. In case of the open-loop control system, control inputs are calculated by the quad-rotor dynamic model and thrust system model that are identified by the thrust test. The 6-DOF real-time simulation environment was constructed in order to verify the performances of attitude controllers.

**Key words:** Quad-Rotor UAV, Flip Maneuver, Open-loop control, 6-DOF Real-time Simulation

## 1. Introduction

In recent years, the small UAV market has grown rapidly. Small UAVs are applied in various areas such as surveillance, reconnaissance, and aerial photography. In this small UAV market, many studies are underway especially for the Quad-rotor. The Quad-rotor unmanned aerial vehicle is one that uses four rotors, which are equipped on the tips of cross-shaped rods.

In addition, Quad-rotor aggressive maneuver researches are actively underway as well, with the aid of motion capture technology, which is a recent technology in this area [1-4]. In case of small UAVs, MEMS gyro sensors are used in many small UAVs, but MEMS gyro sensors have disadvantages that the error signal accumulates during the integration of measured data. However, position and attitude data can be measured with very high accuracy using the motion capture system, so that the system is capable of showing more precise control performance.

The GRASP laboratory of University of Pennsylvania has conducted aggressive maneuvers such as perching, or flips maneuvers. They used three different types of controllers

for performing these maneuvers, and those controllers are categorized as an attitude control, a hover control, and a three-dimensional trajectory follow control. In other words, at one point, only one controller is used to control the Quad-rotor system for each specific condition. When another condition for the Quad-rotor is met, then the controller switching logic is activated to switch the main controller to a different type of controller that is appropriate for the given condition [1].

In addition to this, the ACL at MIT has performed aggressive maneuvers with the variable pitch Quad-rotor [2].

This paper is composed as follows. First of all, the Quad-rotor dynamic model is derived, and an appropriate control system is designed for the dynamic model of the Quad-rotor. We use the conventional PD control method and sliding mode control method for the closed-loop control structure, and calculate input parameters for the open-loop control structure. To perform 6-DOF real time simulations, we assumed that the Quad-rotor flies in an indoor facility equipped with the motion capture system. Therefore we can also assume that measured position and attitude data of the Quad-rotor are very accurate.

This is an Open Access article distributed under the terms of the Creative Commons Attribution Non-Commercial License (<http://creativecommons.org/licenses/by-nc/3.0/>) which permits unrestricted non-commercial use, distribution, and reproduction in any medium, provided the original work is properly cited.

© \* Ph. D Student, Corresponding author: bylee@fdcl.kaist.ac.kr  
\*\* Ph. D Student  
\*\*\* Professor

## 2. Dynamic Modeling of the Quad-Rotor

### 2.1 Quad-Rotor Configuration

The Quad-rotor structure is shown in Fig. 1. This Quad-rotor structure contains four rotors which are mounted on the tip of cross-shaped rods [5].

As we can see from Fig. 1, four rotors are defined as rotor number 1, 2, 3, and 4 in a clockwise direction from the front of the Quad-rotor. Quad-rotor Euler angles are changed by applying the angular velocity differences on these four rotors. We define the angular velocities of four rotors as  $\Omega_1$ ,  $\Omega_2$ ,  $\Omega_3$ , and  $\Omega_4$ , and this actuator system is modeled as the first order system. The Equations (1) represent this actuator system.  $K_t$  is the motor thrust coefficient and  $K_r$  is the motor torque coefficient. Therefore, force  $T$  and torque  $\tau_r$  can be determined by Equations (1).

$$\begin{aligned} T &= K_t \Omega_i^2 \\ \tau_r &= K_r \Omega_i^2 \end{aligned} \quad (1)$$

There are four rotors on the Quad-rotor, so forces acting in each direction of the Quad-rotor are expressed in Equations (2).

$$\begin{aligned} F_x &= 0 \\ F_y &= 0 \\ F_z &= -K_t(\Omega_1^2 + \Omega_2^2 + \Omega_3^2 + \Omega_4^2) \end{aligned} \quad (2)$$

The moments acting on each angular direction of the Quad-rotor are shown in Equations (3), and these equations are considering the gyroscopic effect.

$$\begin{aligned} L &= K_t(-\Omega_2^2 + \Omega_4^2)d - I_r q(\Omega_1 - \Omega_2 + \Omega_3 - \Omega_4) \\ M &= K_t(\Omega_1^2 + \Omega_3^2)d + I_r p(\Omega_1 - \Omega_2 + \Omega_3 - \Omega_4) \\ N &= K_r(-\Omega_1^2 + \Omega_2^2 - \Omega_3^2 + \Omega_4^2) \end{aligned} \quad (3)$$

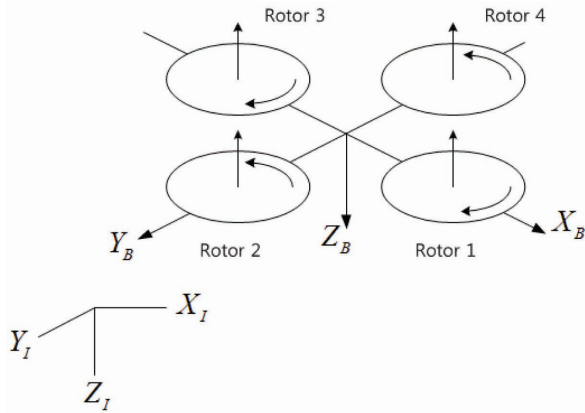


Fig. 1. Quad-rotor configuration

### 2.2 Quad-Rotor Control Allocation

Typically, rotorcraft control commands can be determined as  $\delta_\phi$ ,  $\delta_\theta$ ,  $\delta_\psi$  and  $\delta_z$ .  $\delta_\phi$ ,  $\delta_\theta$ ,  $\delta_\psi$  are the rotor angular velocity differences that generate each-axis torque of the Quad-rotor. Likewise,  $\delta_z$  is the rotor angular velocity difference that generates the vertical direction force of the Quad-rotor. In addition, control allocation is required for converting typical rotorcraft control commands to a rotor's angular velocity commands. The Equations (4) represent the control allocation logic of the Quad-rotor.

$$\begin{aligned} \Omega_1 &= \Omega_{nom} + (\delta_z / 4) + (\delta_\phi / 2) - (\delta_\psi / 4) \\ \Omega_2 &= \Omega_{nom} + (\delta_z / 4) - (\delta_\phi / 2) + (\delta_\psi / 4) \\ \Omega_3 &= \Omega_{nom} + (\delta_z / 4) - (\delta_\phi / 2) - (\delta_\psi / 4) \\ \Omega_4 &= \Omega_{nom} + (\delta_z / 4) + (\delta_\phi / 2) + (\delta_\psi / 4) \end{aligned} \quad (4)$$

## 3. Control System Design

### 3.1 Open Loop Attitude Control

Attitude control is for tracking and maintaining the Euler angles of the Quad-rotor. In this paper, three methods are used for designing the attitude controller. First of all, we use the open-loop control method for designing the attitude controller. To control the attitude of the Quad-rotor, one needs to generate system torques by controlling the angular velocity of each rotor, and the attitude rate of the Quad-rotor should be near zero when the Quad-rotor reaches the desired attitude. Since this method does not use any feedback control, this method is called the open-loop attitude control.

For this purpose, the system torque acting on the Quad-rotor is divided into three stages: acceleration stage, deceleration stage, and stabilization stage. During the acceleration stage, the Quad-rotor angular velocity should be accelerated to the maximum value. In contrast,

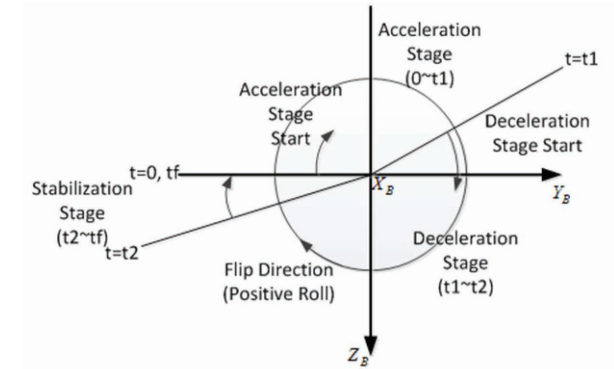


Fig. 2. Sequence of Flip Maneuver using Open-loop control method

in the deceleration stage, the Quad-rotor angular velocity should be decelerated to the minimum value. Finally, in the stabilization stage, all rotors should rotate in the same angular velocities in order for the Quad-rotor to return safely to the original hovering state.

One good application is to consider the Quad-rotor performing a positive roll flip maneuver. We assume that the gyroscopic effect and disturbance are small enough to be negligible. A graphical representation for each stage of the flip maneuver is illustrated in Fig. 2. Before conducting the open-loop attitude control, the Quad-rotor should hold the hover state, then all rotors should rotate with the identical nominal angular velocity,  $\Omega_{nom}$ . We have already assumed that the gyroscopic effect and disturbance are negligible, so that there is no system torque on the pitch axis in all stages. Therefore, rotors 1 and 2 hold their angular velocities as  $\Omega_{nom}$  in all stages.

In acceleration and deceleration stages, the torques and differences of angular velocities and Euler angles are as follows. In the acceleration stage, the angular velocity of rotor 2 decreases whereas the angular velocity of rotor 4 increases. Rotor 2 should rotate with the minimum angular velocity,  $\Omega_{min}$ , and rotor 4 should rotate in the maximum angular velocity,  $\Omega_{max}$ . Maximum and minimum angular velocities,  $\Omega_{max}$  and  $\Omega_{min}$  can be obtained as Equations (5).

$$\begin{aligned} \Omega_{max} &= \Omega_{nom} + \Delta\Omega_{max} \\ \Omega_{min} &= \Omega_{nom} - \Delta\Omega_{min} \end{aligned} \quad (5)$$

where  $\Delta\Omega_{max}$  and  $\Delta\Omega_{min}$  represent the changes in maximum and minimum angular velocity, respectively. In this paper, we assume that  $\Delta\Omega_{min} = \Delta\Omega_{max}$ , and it indicates that there is no extra torque generated from the flip maneuver except for the roll torque. In addition, the hovering stage, acceleration stage, deceleration stage, and stabilization stage are numbered as stages zero, one, two, and three, respectively. Now, in the  $x$ -th stage, angular velocities of rotor 2 and rotor 4 are denoted as  $\Omega_{2,x}$  and  $\Omega_{4,x}$ , and the angular velocity variations during the  $x$ -th stage are denoted as  $\Delta\Omega_x$ . Accordingly, angular velocities of rotor 2 and rotor 4 are expressed in Equations (6).

$$\begin{aligned} \Omega_{2,x} &= \Omega_{2,x-1} - \Delta\Omega_x \\ \Omega_{4,x} &= \Omega_{4,x-1} + \Delta\Omega_x \end{aligned} \quad (6)$$

Angular velocity variations in the  $x$  stage and angular velocities of rotor 2 and rotor 4 in the  $x-1$  stage can be found in Table 1.

In this paper, the rotor system is modeled as a first order system with a time constant  $\tau$ . Therefore, the angular velocity of rotor 2 during the flip maneuver is expressed in Equation (7).

$$\begin{aligned} \Omega_2(t) &= \Omega_{nom} - \Delta\Omega_{max} (1 - e^{-\frac{t-t_0}{\tau}}) u_{t_0} \\ &\quad + 2\Delta\Omega_{max} (1 - e^{-\frac{t-t_1}{\tau}}) u_{t_1} \\ &\quad - \Delta\Omega_{max} (1 - e^{-\frac{t-t_2}{\tau}}) u_{t_2} \end{aligned} \quad (7)$$

$$\begin{aligned} \Omega_4(t) &= \Omega_{nom} + \Delta\Omega_{max} (1 - e^{-\frac{t-t_0}{\tau}}) u_{t_0} \\ &\quad - 2\Delta\Omega_{max} (1 - e^{-\frac{t-t_1}{\tau}}) u_{t_1} \\ &\quad + \Delta\Omega_{max} (1 - e^{-\frac{t-t_2}{\tau}}) u_{t_2} \end{aligned} \quad (8)$$

The angular velocity of rotor 4,  $\Omega_4(t)$ , is similar to that of Equation (8), but all the signs are opposite. System torque acting on the Quad-rotor's roll-axis is expressed in Equation (9).

$$L = K_l (-\Omega_2^2 + \Omega_4^2) d \quad (9)$$

Moment  $L_x(t)$  acting on the Quad-rotor at stage  $x$  is expressed in Equation (10).

$$L_x(t) = K_l d (-\Omega_{2,x-1}^2 + \Omega_{4,x-1}^2 + 2(\Omega_{2,x-1} + \Omega_{4,x-1})\Delta\Omega_x (1 - e^{-\frac{t-t_{x-1}}{\tau}}) u_{t_{x-1}}(t)) \quad (10)$$

Now, the moment sum during whole flip maneuver is defined as  $L_{flip}(t)$ , and  $L_{flip}(t)$  can be derived by Equations (7), (8) and (9).  $L_{flip}(t)$  is expressed in Equation (11).

$$L_{flip}(t) = 4K_l d \Omega_{nom} \Delta\Omega_{max} ((1 - e^{-\frac{t-t_0}{\tau}}) u_{t_0}(t) - 2(1 - e^{-\frac{t-t_1}{\tau}}) u_{t_1}(t) + (1 - e^{-\frac{t-t_2}{\tau}}) u_{t_2}(t)) \quad (11)$$

We defined the Quad-rotor's angular acceleration during the flip maneuver as  $\alpha_{pflip}(t)$ . Therefore,  $\alpha_{pflip}(t)$  can be

Table 1. Parameters of Open-loop control for each Stage

Stage (x)	Acc. (1)	Dec. (2)	Sta. (3)
$t_x$	$t_0 \sim t_1$	$t_1 \sim t_2$	$t_2 \sim t_f$
$\Omega_{2,x-1}$	$\Omega_{nom}$	$\Omega_{nom} - \Delta\Omega_{max}$	$\Omega_{nom} + \Delta\Omega_{max}$
$\Omega_{4,x-1}$	$\Omega_{nom}$	$\Omega_{nom} + \Delta\Omega_{max}$	$\Omega_{nom} - \Delta\Omega_{max}$
$\Delta\Omega_x$	$\Delta\Omega_{max}$	$-2\Delta\Omega_{max}$	$\Delta\Omega_{max}$

obtained from Equation (11) and inertia of the Quad-rotor.  $\alpha_{pflip}(t)$  is expressed in Equation (12).

$$\alpha_{pflip}(t) = \frac{1}{I_x} L_{flip}(t) \quad (12)$$

In addition, we can obtain angular velocities and Euler angles of the Quad-rotor at time  $t$  by integrating  $\alpha_{pflip}(t)$  with respect to time. Angular velocities and Euler angles of the Quad-rotor are denoted as  $p_{flip}(t)$  and  $\phi_{flip}(t)$ . Finally, terminal condition of  $\alpha_{pflip}(t)$ ,  $p_{flip}(t)$ , and  $\phi_{flip}(t)$  will be decided. In other words, when the open-loop attitude control is finished, the allowable errors of the angular acceleration are defined as  $\pm E_{\alpha_p} \text{ rad/sec}^2$ . In the same manner, allowable errors of the angular velocities at that specific moment are defined as  $\pm E_p \text{ rad/sec}$ . In case of flip maneuver, terminal condition of the roll angle is 360 degrees. These terminal conditions are expressed in Equations (13). Now, we can calculate  $t_1$  and  $t_2$  that satisfy the terminal condition. Then, it leads to a successful calculation of the control input for the open-loop

flip maneuver.

$$\begin{aligned} -E_{\alpha_p} &\leq \alpha_p(t_f) \leq E_{\alpha_p} \\ -E_p &\leq p(t_f) \leq E_p \\ \phi(t_f) &= 2\pi \end{aligned} \quad (13)$$

We built the Quad-rotor frame to determine parameters of the open-loop attitude control method. This frame is based on Mikrokopter Company's Quad-rotor frame, and it is shown in Fig. 3.

Quad-rotor parameters are determined by measured data and calculated data using a previously built Quad-rotor frame as shown in Table 2.

The thrust system of the Quad-rotor frame is composed of a propeller, motor, ESC and battery. The Thrust test was performed in order to measure the thrust coefficient and torque coefficient of the thrust system. The test environment has been set up as shown in Fig. 4. At this time, the rotor thrusts are measured by load cell, and the angular velocity

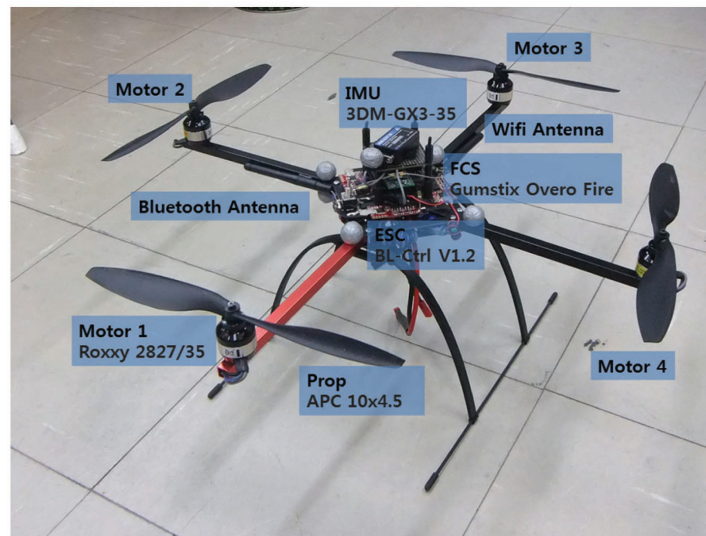


Fig. 3. Quad-rotor Frame Structure

Table 2. Quad-rotor Parameters

Parameter	Description	Value	Unit
$m$	Mass	1.145	kg
$I_r$	Rotor Inertia	$5.142 \times 10^{-4}$	$kg \cdot m^2$
$I_x$	Moment of Inertia (X-axis)	$9.618 \times 10^{-3}$	$kg \cdot m^2$
$I_y$	Moment of Inertia (Y-axis)	$9.766 \times 10^{-3}$	$kg \cdot m^2$
$I_z$	Moment of Inertia (Z-axis)	$1.843 \times 10^{-2}$	$kg \cdot m^2$
$d$	Distance (motor to c.g)	0.225	m

of the rotor are measured by the laser sensor simultaneously.

By observing the thrust test results, the thrust coefficient is determined as  $K_f=1.764 \times 10^{-5} (N/(rad/sec)^2)$  and torque coefficient is determined as  $K_t=2.547 \times 10^{-7} (N \cdot m/(rad/sec)^2)$ . In addition to this, system identification was performed in order to obtain the thrust system model. From these results, parameters of the thrust system are determined such as table 3.

Now, we are going to calculate time  $t_1$  and  $t_2$  that satisfy Equations (13). For this purpose, we determined the parameters of Equations (13) as  $E_{\alpha_p}=0.1 rad/sec^2$ ,  $E_p=0.1 rad/sec$ . Therefore, we can obtain calculated results,  $t_1=0.196 sec$ ,  $t_2=0.392 sec$  and  $t_f=1.462 sec$ . Simulation results without gyroscopic effect are presented in Fig. 5. As we can observe from Fig. 5, the Quad-rotor's angular velocity  $p$  is increasing to  $\alpha_p$  and the Quad-rotor's angular acceleration  $1000 deg/sec$  is increasing to  $6000 deg/sec^2$ .

### 3.2 PD Attitude Control

In this subsection, we use the PD control method for designing the attitude controller. Equations and structure of the PD attitude controller are shown in Equations (14) and Fig. 6.

$$\begin{aligned} \delta_\phi &= K_{d,\phi}(K_{p,\phi}(\phi_{cmd} - \phi) - p) \\ \delta_\theta &= K_{d,\theta}(K_{p,\theta}(\theta_{cmd} - \theta) - q) \\ \delta_\psi &= K_{d,\psi}(K_{p,\psi}(\psi_{cmd} - \psi) - r) \end{aligned} \tag{14}$$

### 3.3 Sliding Mode Attitude Control

We can use the sliding mode control to conduct the Quad-rotor's aggressive maneuvers. A brief introduction of the sliding model control is presented below [6-8]. Tracking error  $\tilde{\mathbf{x}}$  is defined in Equation (15).

$$\tilde{\mathbf{x}} = \mathbf{x} - \mathbf{x}_d = [\tilde{\phi} \quad \tilde{\theta} \quad \tilde{\psi} \quad \tilde{p} \quad \tilde{q} \quad \tilde{r}]^T \tag{15}$$

At this time, sliding surface  $s$  is defined by Equation (16).

$$s = \begin{bmatrix} s_1 \\ s_2 \\ s_3 \end{bmatrix} = \begin{bmatrix} \lambda_\phi & 0 & 0 & 1 & 0 & 0 \\ 0 & \lambda_\theta & 0 & 0 & 1 & 0 \\ 0 & 0 & \lambda_\psi & 0 & 0 & 1 \end{bmatrix} \tilde{\mathbf{x}} = \begin{bmatrix} \lambda_\phi \tilde{\phi} + \dot{\tilde{\phi}} \\ \lambda_\theta \tilde{\theta} + \dot{\tilde{\theta}} \\ \lambda_\psi \tilde{\psi} + \dot{\tilde{\psi}} \end{bmatrix} \tag{16}$$

If  $s=0$ , then we can derive Equations (17) using Equation (15).

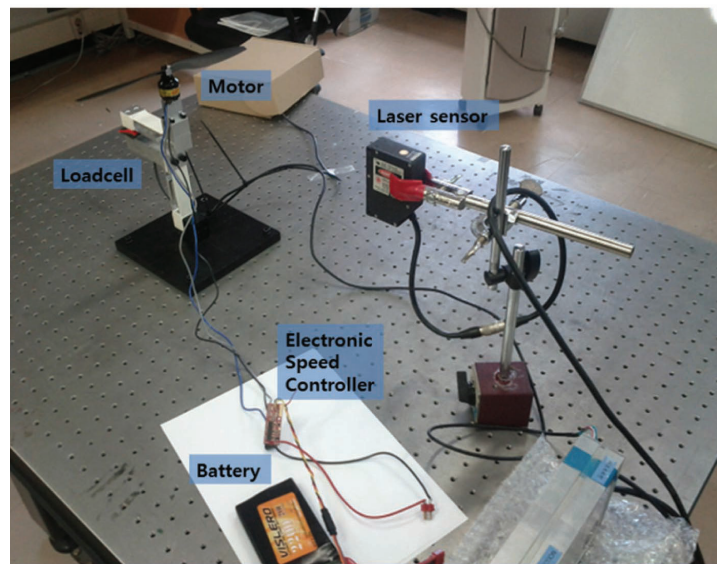


Fig. 4. Thrust test setting or single motor

Table 3. Parameters of Thrust Models

Equation	$T_d$	$\frac{1}{a}$	$\zeta$	$\frac{1}{\omega_n}$
$\frac{1}{s+a} \times e^{-T_d s}$	0.02	0.155	.	.

$$\begin{aligned}
 s_1 &= \lambda_\phi \tilde{\phi} + \dot{\tilde{\phi}} = 0 \\
 s_2 &= \lambda_\theta \tilde{\theta} + \dot{\tilde{\theta}} = 0 \\
 s_3 &= \lambda_\psi \tilde{\psi} + \dot{\tilde{\psi}} = 0
 \end{aligned}
 \tag{17}$$

If  $\lambda_\phi$ ,  $\lambda_\theta$  and  $\lambda_\psi$  are greater than zero, then  $\tilde{\mathbf{x}}$  and  $\dot{\tilde{\mathbf{x}}}$  have the opposite sign, therefore we know that the sliding surface will converge to zero. Now, to make  $s=0$ , we define control law  $u(t)$  as in Equation (18).

$$u(t) = -K_s \frac{s(t)}{\|s(t)\|} - K_p s(t)
 \tag{18}$$

Here,  $K_s$  is the gain of the sign function of the  $s$ , and  $K_p$  is the gain of the proportional component of the  $s$ .

## 4. Simulation

### 4.1 Attitude Control Simulation using Open Loop Attitude Control

In this subsection, we perform the flip maneuver simulation using the open-loop control that we introduced in section 3.1. Parameters for the open-loop control are the

same as those introduced in section 3.1. Simulation results of the Euler angles are shown in Fig. 7, and Simulation results of angular velocities are shown in Fig. 8. As we can observe in Fig. 7, the Quad-rotor's Euler angle  $\phi$  is reaching 360 degrees with a fast rise time. At this time, rise time is approximately 0.43 seconds, but Euler angle  $\phi$  diverges eventually.

There are many reasons why the Euler angle  $\phi$  diverges, but one of the main reasons is that the parameter values were calculated without the gyroscopic effect. This gyroscopic effect will make an unintended change to the Euler angles. However, the open-loop controller does not have feedback so it cannot compensate this disturbance. Due to these reasons, Euler angles diverge during the flip maneuver with the open-loop control method.

### 4.2 Attitude Control Simulation using PD Attitude Control

In this subsection, we use the PD attitude controller to simulate the flip maneuver. Simulation results of Euler angles are shown in Fig. 9, and simulation results of angular velocities are shown in Fig. 10. From the simulation results, the PD attitude controller takes about two seconds to accomplish the flip maneuver. We also know that maximum

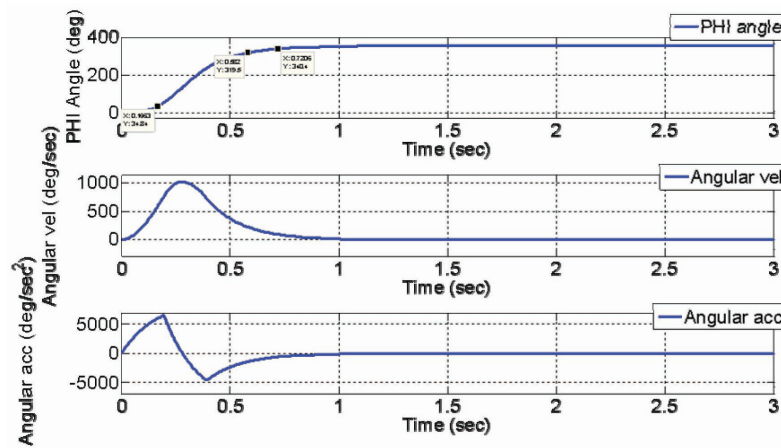


Fig. 5. Simulation results of open-loop flip maneuver without gyroscopic effect

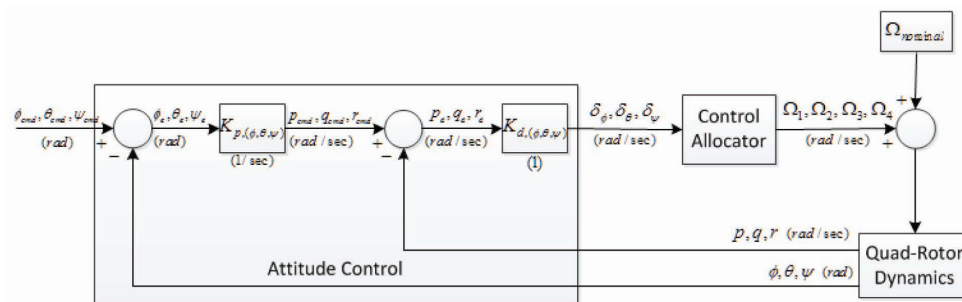


Fig. 6. PD Attitude Control

$p$  is approximately 350 deg/sec. As we can observe from the simulation results graph, rise time is about 1.17 seconds and settling time is about 1.64 seconds. Comparing these results with the simulation results of the open-loop flip maneuver that we described in section 4.1, we find that the accomplish time for the flip maneuver of the PD attitude controller is remarkably slower than using the open-loop control results. However, simulation results of Fig. 5 do not consider the gyroscopic effect, so these results do not represent all simulation results of the open-loop control.

### 4.3 Attitude Control Simulation using Sliding Mode Attitude Control

In this subsection, simulation results of the flip maneuver using sliding mode control will be presented. Parameters of sliding mode control such as  $S$ ,  $K_s$  and  $K_p$ , are determined in Table 4.

Simulation results of Euler angles are shown in Fig. 11. Simulation results of angular velocities are shown in Fig. 12.

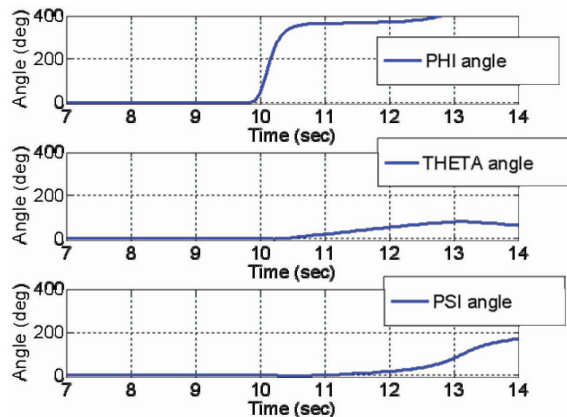


Fig. 7. Attitude Control Simulation Results of Euler Angle with Open-loop control

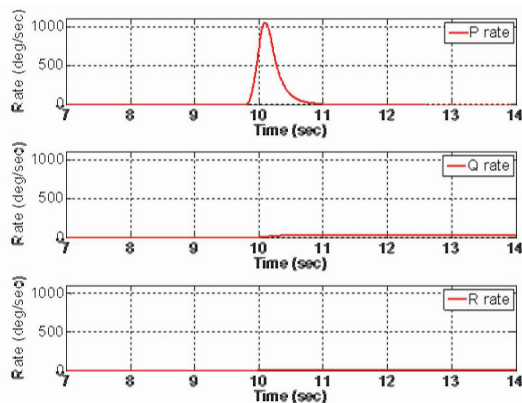


Fig. 8. Attitude Control Simulation Results of Angular Velocity with Open-loop control

As we can observe in Fig. 11, rise time of sliding mode control is approximately 0.58 seconds and settling time is about 0.93 seconds. Angular velocity  $p$  reaches up to 600 deg/sec. In case of sliding mode control, rise time and settling time are faster than using the PD control method, but overshoot does not have large differences between the sliding mode control method and PD control method. In contrast, in case of sliding mode control, even though rise time and settling time are slower than using the open-loop control method, it has an advantage that the response from SMC method does not diverge during the flip maneuver. The sliding mode control method also has disadvantages that there is a chattering effect when sliding surface  $s$  is equal to zero. We can observe the chattering effect in Fig. 11.

### 4.4 Performance Comparison of Attitude Controllers

Until now, we performed high angle control using three attitude controllers. Characteristics of these controllers are listed in Table 5.

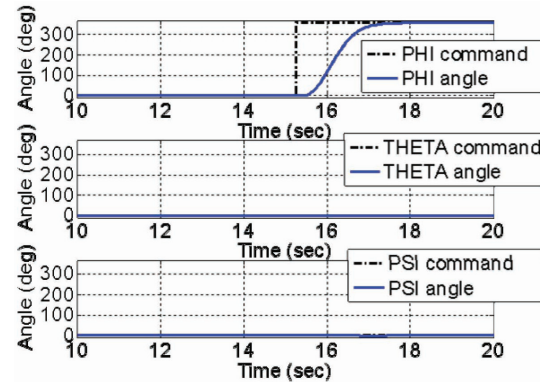


Fig. 9. Attitude Control Simulation Results of Euler Angle with PD Control

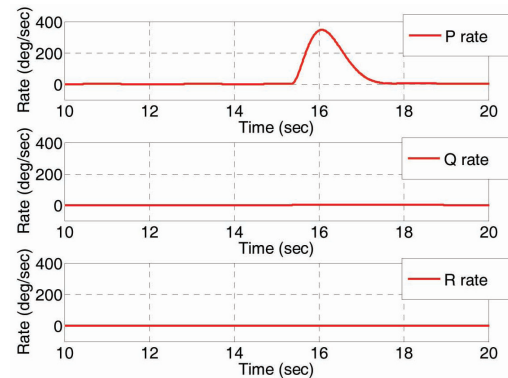


Fig. 10. Attitude Control Simulation Results of Angular Velocity with PD Control

### 5. Conclusion

In this paper, three attitude controllers of the Quad-rotor were designed by various methodologies to perform a flip maneuver and we also compared performances of these attitude controllers. For this purpose, 6-DOF dynamic equations were derived and the Quad-rotor frame was configured. Here, we assumed that the aerodynamic components are small enough to be negligible. To control the attitude of the Quad-rotor, we designed three types of controllers. First, the open-loop controller was designed for the attitude control and the conventional PD controller was designed second. Lastly, the sliding mode control method was used to design the attitude control of the Quad-rotor. We simulated a flip maneuver using these three attitude controllers and compared performances of these attitude controllers. In case of the open-loop control

system, convergence speed is fast, but failed to hold the stability of the system. In contrast, the PD control system satisfies successful stabilization of the Quad-rotor with one drawback: convergence speed is slower than that of the open-loop control system. Finally, the sliding mode control system satisfies both convergence speed and stabilization. However, we can observe that there is chattering effect when sliding surface  $s$  is equal to zero. To perform the flight test in the subsequent study, we built the Quad-rotor frame and we also modeled it to determine the parameters of the Quad-rotor.

### Acknowledgement

This research was supported by Defense Acquisition Program Administration and Agency for Defense

Table 4. Parameters of Sliding Mode Control (Simulation)

$S$	$K_s$	$K_p$
$\begin{bmatrix} 1 & 0 & 0 & 0.58 & 0 & 0 \\ 0 & 1 & 0 & 0 & 0.58 & 0 \\ 0 & 0 & 3 & 0 & 0 & 3.5 \end{bmatrix}$	$\begin{bmatrix} 10 & 0 & 0 \\ 0 & 10 & 0 \\ 0 & 0 & 20 \end{bmatrix}$	$\begin{bmatrix} 20 & 0 & 0 \\ 0 & 20 & 0 \\ 0 & 0 & 20 \end{bmatrix}$

Table 5. Performance Comparisons of Three Attitude Controllers

	Open-loop	PD	Sliding Mode
<b>Rising Time (sec)</b>	0.43	1.17	0.58
<b>Settling Time (sec)</b>	X	1.64	0.93
<b>Advantage</b>	Fast rise time	Stable	Fast settling time
<b>Disadvantage</b>	No feedback loop	Slow settling time	Chattering

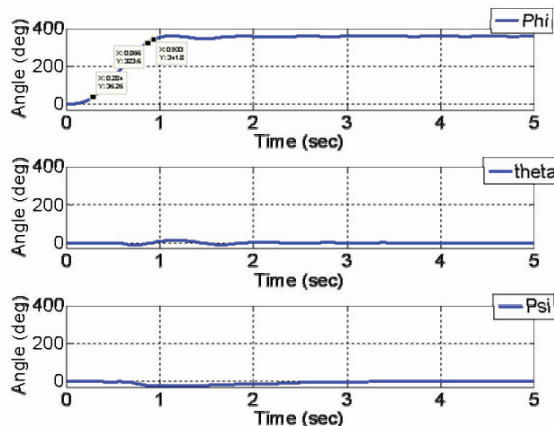


Fig. 11. Attitude Control Simulation Results of Euler Angle with Sliding Mode Control

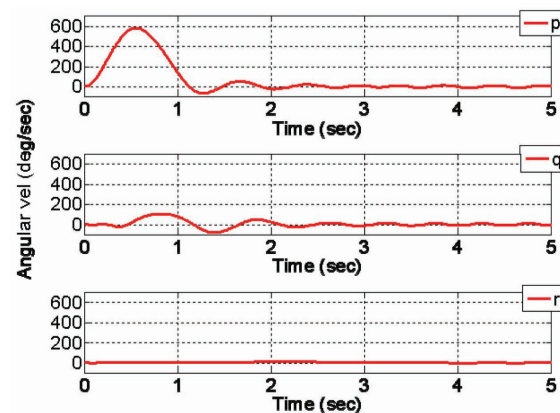


Fig. 12. Attitude Control Simulation Results of Angular Velocity with Sliding Mode Control

Development under the contract UE124026JD.

## References

- [1] Mellinger, D., Michael, N., and Kumar, V., "Trajectory generation and control for precise aggressive maneuvers with quadrotors," *The International Journal of Robotics Research*, Vol. 31, No. 5, 2012, pp. 664-674.
- [2] Cutler, M., Ure, N. K., Michini, B., and How, J. P., "Comparison of Fixed and Variable Pitch Actuators for Agile Quadrotors," *AIAA Guidance, Navigation and Control Conference*, Portland, OR, 2011.
- [3] Lupashin, S., and D'Andrea, R., "Adaptive fast open-loop maneuvers for quadcopters," *Autonomous Robots*, Vol 33, 2012, pp. 89-102.
- [4] Schoellig, A. P., Mueller, F. L., and D'Andrea, R., "Optimization-based iterative learning for precise quadcopter trajectory tracking," *Autonomous Robots*, Vol 33, 2012, pp. 103-127.
- [5] Bresciani, T., "Modelling, Identification and Control of a Quadrotor Helicopter," *Master Thesis*, Lund University, Lund, Sweden, 170 pages, 2008.
- [6] Monsees, G., "Discrete-Time Sliding Mode Control," *Ph.D Thesis*, Delft University of Technology, Delft, Netherlands, 2002.
- [7] Won, D. Y., and Tahk, M. J., "Sliding Mode Controller Design for Quad-Rotor Attitude Stabilization," *3rd TokyoTech-KAIST Joint Workshop for Mechanical Engineering Students*, 2007.
- [8] Slotine, J. E., and Li, W., *Applied Nonlinear Control*, Prentice-Hall International, Inc, City, 1991.